GUT MICROBIOTA

Histamine production by the gut microbiota induces visceral hyperalgesia through histamine 4 receptor signaling in mice

Giada De Palma[1]†, Chiko Shimbori[1]†, David E. Reed[2]†, Yang Yu[2], Virginia Rabbia[1], Jun Lu[1], Nestor Jimenez-Vargas[2], Jessica Sessenwein[2], Cintya Lopez-Lopez[2], Marc Pigrau[1], Josue Jaramillo-Polanco[2], Yong Zhang[2], Lauren Baerg[1], Ahmad Manzar[1], Julien Pujo[1], Xiaopeng Bai[1], Maria Ines Pinto-Sanchez[1], Alberto Caminero, Karen Madsen[3], Michael G. Surette[1], Michael Beyak[2], Alan E. Lomax[2], Elena F. Verdu[1], Stephen M. Collins[1], Stephen J. Vanner[2]‡, Premysl Bercik[1]*‡

The gut microbiota has been implicated in chronic pain disorders, including irritable bowel syndrome (IBS), yet specific pathophysiological mechanisms remain unclear. We showed that decreasing intake of fermentable carbohydrates improved abdominal pain in patients with IBS, and this was accompanied by changes in the gut microbiota and decreased urinary histamine concentrations. Here, we used germ-free mice colonized with fecal microbiota from patients with IBS to investigate the role of gut bacteria and the neuroactive mediator histamine in visceral hypersensitivity. Germ-free mice colonized with the fecal microbiota of patients with IBS who had high but not low urinary histamine developed visceral hyperalgesia and mast cell activation. When these mice were fed a diet with reduced fermentable carbohydrates, the animals showed a decrease in visceral hypersensitivity and mast cell accumulation in the colon. We observed that the fecal microbiota from patients with IBS with high but now low urinary histamine produced large amounts of histamine in vitro. We identified *Klebsiella aerogenes*, carrying a histidine decarboxylase gene variant, as a major producer of this histamine. This bacterial strain was highly abundant in the fecal microbiota of three independent cohorts of patients with IBS compared with healthy individuals. Pharmacological blockade of the histamine 4 receptor in vivo inhibited visceral hypersensitivity and decreased mast cell accumulation in the colon of germ-free mice colonized with the high histamine-producing IBS fecal microbiota. These results suggest that therapeutic strategies directed against bacterial histamine could help treat visceral hyperalgesia in a subset of patients with IBS with chronic abdominal pain.

INTRODUCTION

The gut microbiota has been implicated in the genesis of some chronic pain disorders, including pain associated with irritable bowel syndrome (IBS) and fibromyalgia (*1*–*3*). This is largely based on clinical associations between pain and altered gut microbiota profiles found in clinical studies, differences in pain thresholds between conventionally raised and germ-free mice that normalized after bacterial colonization, or the ability of bacteria to produce neuroactive metabolites in vitro (*4*). However, data demonstrating a causal link and precise mechanisms underlying gut microbiota–induced visceral pain, as well as identification of the specific bacterial species involved, are lacking.

We previously reported that abdominal pain in patients with IBS improved after restricting ingestion of fermentable carbohydrates in the diet. This was associated with changes in gut microbiota profiles and lower concentrations of urinary histamine (*2*), a known mediator involved in visceral hypersensitivity (*5*–*7*). Here, we investigated gut microbial pathways that trigger histamine production and visceral hypersensitivity using germ-free mice colonized with the fecal microbiota of patients with IBS or healthy individuals (*8*).

[1]Farncombe Family Digestive Health Research Institute, McMaster University, Hamilton, Canada. [2]Gastrointestinal Diseases Research Unit, Queens University, Kingston, Canada. [3]University of Alberta, Edmonton, Canada.
*Corresponding author. Email: bercikp@mcmaster.ca
†These first authors contributed equally to this work.
‡These senior authors contributed equally to this work.

RESULTS

Gut microbiota transplantation from patients with IBS with high urinary histamine into germ-free mice induces visceral hyperalgesia

A reanalysis of data from our trial of a low fermentable carbohydrate diet in patients with IBS (*2*) found a moderate correlation ($r = 0.44$, $P = 0.009$) between visceral pain severity and the concentration of urinary histamine (Fig. 1A). Although in some patients with IBS urinary histamine was low or unmeasurable, it was elevated in one-third of this IBS cohort, suggesting that histamine could be involved in nociception in this subset of patients.

To investigate whether gut microbial species could contribute to increased urinary histamine concentrations and visceral hyperalgesia, we colonized germ-free mice (total $n = 34$, using at least two mice per donor) with fecal microbiota samples from five patients with IBS with high urinary histamine and five patients with IBS with low urinary histamine (see table S1 for patient demographics). Mice were fed a custom-designed high fermentable carbohydrate diet (table S2) and were examined 3 weeks later. We found that intestinal mechanosensitivity, assessed by measuring action potential discharge in single afferent nerves of the colon, was higher in germ-free mice colonized with the fecal microbiota of patients with IBS with high urinary histamine compared with low urinary histamine ($P = 0.005$) (Fig. 1B).

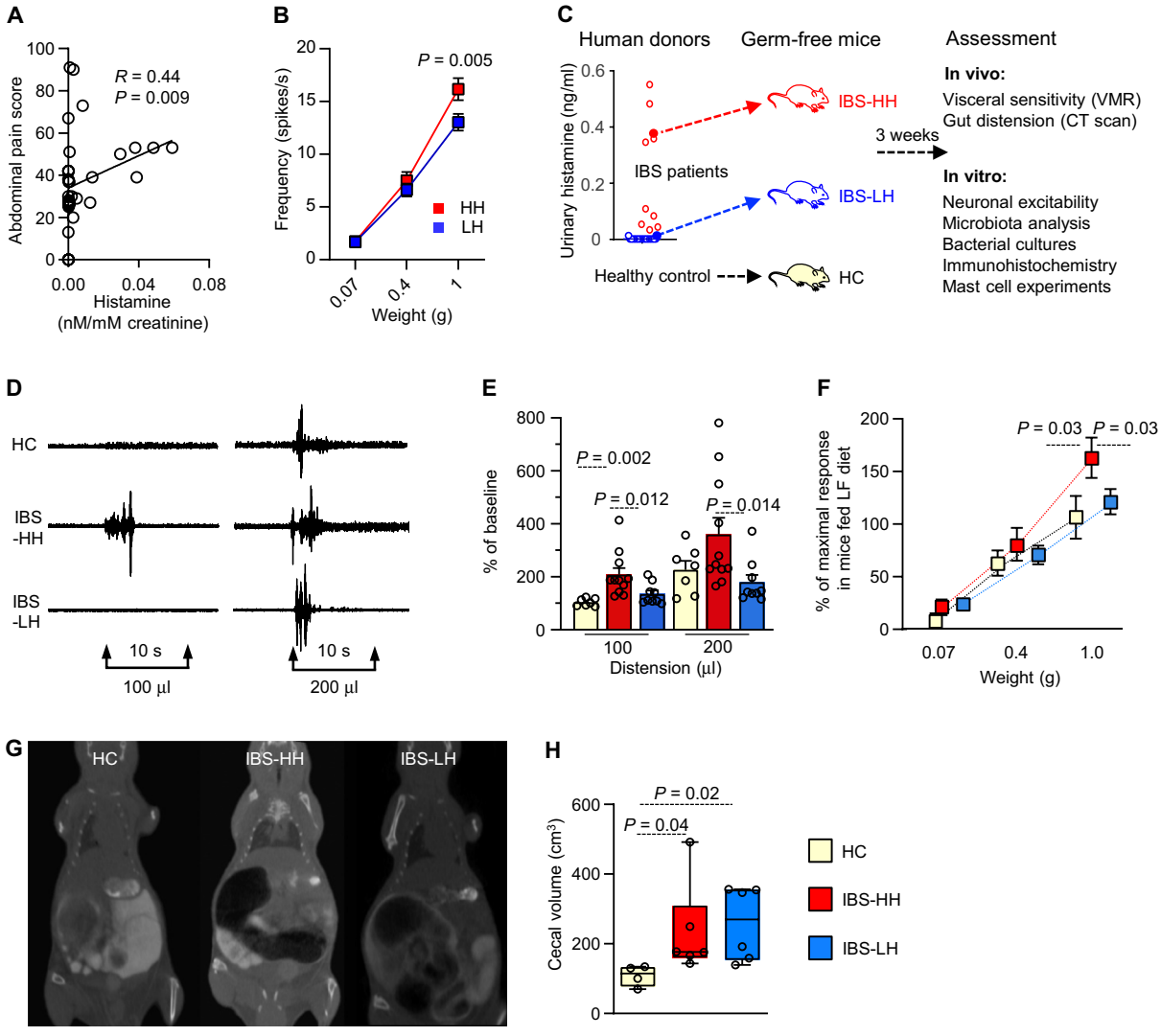

Fig. 1. Germ-free mice colonized with fecal microbiota from patients with IBS with high urinary histamine exhibit visceral hypersensitivity. (**A**) Data from a prior clinical study in patients with IBS investigating the effect of a high or low fermentable diet (*2*) were reanalyzed. The relationship between abdominal pain and urinary histamine concentration was examined. Abdominal pain correlated with urine histamine concentration in patients with IBS ($n = 34$). (**B**) Mechanosensitivity in single afferent nerves was measured in germ-free mice transplanted with fecal microbiota from patients with IBS with high (HH, $n = 5$) or low (LH, $n = 5$) urinary histamine concentrations ($n = 5$ mice per group). Recordings were from at least 53 single afferent units per mouse group, with a minimum of 3 U per mouse. Each unit was probed using the vFH test with weights of 0.07, 0.4, and 1.0 g. (**C**) Shown is the experimental design for mechanistic studies involving colonization of germ-free mice with fecal microbiota from a patient with IBS with either high (IBS-HH, red) or low (IBS-LH, blue) urine histamine concentrations or from a healthy control (HC, yellow). In vivo and in vitro assessments commenced 3 weeks after fecal microbiota transplant. (**D**) Shown are representative traces of visceromotor responses (VMR) to colorectal distension of 100 µl or 200 µl in conscious mice colonized with fecal microbiota from a patient with IBS with either high (HH) or low (LH) urinary histamine or a healthy control (HC). (**E**) Shown are visceromotor responses to colorectal distension in mice colonized with fecal microbiota from patients with IBS with high (IBS-HH, $n = 9$) or low (IBS-LH, $n = 9$) urinary histamine or from healthy controls (HC, $n = 7$). (**F**) Mechanosensitivity in single afferent nerves was measured in mice with fecal microbiota transplants from a patient with IBS with high (IBS-HH) ($n = 22$ U) or low (IBS-LH) ($n = 23$ U) urinary histamine or a healthy control (HC) ($n = 9$ U). Each unit was probed with a vFH test with weights of 0.07, 0.4, and 1.0 g. The response was calculated as relative to the maximum response in mice colonized with the same fecal microbiota and fed a low fermentable (LF) diet. (**G**) Shown are representative CT scans of the abdomen of mice colonized with fecal microbiota from a patient with IBS with high (IBS-HH) or low (IBS-LH) urinary histamine or a healthy control (HC). (**H**) Shown are cecum volumes in mice colonized with fecal microbiota from patients with IBS with high (IBS-HH, $n = 6$) or low (IBS-LH, $n = 6$) urinary histamine or healthy controls (HC, $n = 4$). Unless otherwise stated, the data are shown as means ± SEM. Data were analyzed with a one-way (E) or two-way ANOVA (B and F) with Holm-Sidak's correction or Kruskal-Wallis test with Dunn's correction (H). *P* values correspond to post hoc multiple comparisons.

Diet-microbiota interactions underlie visceral hyperalgesia in mice colonized with microbiota from patients with IBS with high urinary histamine

Next, we colonized additional germ-free mice ($n = 119$) with the fecal microbiota from one patient with IBS with high urinary histamine, one patient with IBS with low urinary histamine, and a healthy control individual and then fed the animals a high or low fermentable diet (Fig. 1C and table S2). We also included mice born and raised conventionally, harboring a specific pathogen–free (SPF) gut microbiota, as an additional control group. 16*S* ribosomal RNA

(rRNA) gene sequence analysis demonstrated that mouse gut microbial β-diversity profiles clustered with their human donors (fig. S1A). The gut microbial profiles of mice colonized with stool samples from patients with IBS mirrored the pattern observed in the IBS patient samples (fig. S1, B to E) (*2*), with lower bacterial diversity and lower diversity of Firmicutes and Clostridiales compared with healthy individuals.

We examined visceral sensitivity in conscious mice by recording visceromotor responses to colorectal distension using a custom ambulatory harness containing electromyogram (EMG) recording electrodes and a barostat. Germ-free mice colonized with the fecal microbiota from a patient with IBS with high urinary histamine displayed hyperalgesia compared with animals colonized with the fecal microbiota from a patient with IBS with low urinary histamine or from a healthy control (Fig. 1, D and E). Moreover, in mice colonized with the fecal microbiota from a patient with IBS with high urinary histamine, there was increased firing of colonic afferent nerves in response to mechanical stimulation (Fig. 1F and fig. S2A). A low fermentable diet decreased hyperalgesic responses in these animals but did not affect responses in germ-free mice colonized with fecal microbiota from a healthy control or a patient with IBS with low urinary histamine. A low fermentable diet did not affect pain responses in SPF control mice (fig. S2, A to C).

Neither gut distension nor short-chain fatty acids are drivers of visceral hyperalgesia

As bacterial fermentation with gas production and bowel distension was suggested to mediate abdominal pain in patients with IBS eating a high fermentable carbohydrate diet (*9*, *10*), we used computed tomography (CT) imaging to assess the volume of the mouse cecum, a major site of fermentation. Cecum size was greater in mice colonized with an IBS fecal microbiota compared with a healthy control fecal microbiota; cecum size was similar in all mice colonized with fecal microbiotas from patients with IBS with high or low urinary histamine (Fig. 1, G and H). A low fermentable carbohydrate diet led to a decrease in cecal volume in SPF mice and in germ-free mice colonized with an IBS fecal microbiota but not a healthy control fecal microbiota (fig. S2, D and E).

The bacterial metabolites, butyrate and propionate, have been suggested to affect intestinal neuroimmune function (*11*, *12*), thus possibly influencing visceral sensitivity. However, we found no difference in total short-chain fatty acids (SCFAs), butyrate, or propionate in the cecum of any of the germ-free mice colonized with human fecal microbiotas or in SPF mice when the animals were fed a high fermentable carbohydrate diet (fig. S3, A to C). The low fermentable carbohydrate diet decreased SCFA and butyrate production only in germ-free mice colonized with a healthy control fecal microbiota. Thus, we next investigated histamine, which can be produced by bacteria through the activity of the histidine decarboxylase (*hdc*) gene (*13*, *14*).

The fecal microbiota of patients with IBS with high urinary histamine produces large amounts of histamine

First, we studied gut microbial histamine production by incubating the cecal contents from human microbiota–transplanted mice with excess histidine. The cecum of mice colonized with the fecal microbiota of a patient with IBS with high urinary histamine produced 38 times more histamine than that of mice colonized with microbiota of a patient with IBS with low urinary histamine or a healthy control ($P = 0.03$ and $P = 0.02$, respectively) (Fig. 2A). The low-fermentable carbohydrate diet decreased histamine production in mice colonized with the fecal microbiota from a patient with IBS with high urinary histamine ($P < 0.001$) but had no effect on mice colonized with the fecal microbiota from a patient with IBS with low urinary histamine or a healthy control (fig. S4A). Bacterial histamine abundance moderately correlated with visceral mechanosensitive responses, as assessed by firing of afferent nerves in the colon in response to mechanical stimulation (fig. S4B).

Next, we validated these findings in stool samples from patients with IBS. Stool samples from patients with IBS from our dietary study (*2*) with high urinary histamine produced more histamine than did stool samples from patients with IBS with low urinary histamine ($P = 0.07$) (Fig. 2B). As these stool samples were used previously for several analyses, which possibly affected the viability of bacteria due to repeated freeze-and-thaw cycles, we further explored histamine production and pain reporting in an independent cohort of patients with IBS. These patients (table S3) were followed longitudinally, and their stool samples were collected at periods of high and low abdominal pain. We found that the microbiota in stool samples collected during a period of high pain produced more histamine than did the fecal microbiota from the same patients collected at periods of low or no abdominal pain ($P = 0.009$) (Fig. 2C).

Klebsiella aerogenes is the main histamine producer in patients with IBS

As histamine can be secreted by many bacteria (*13*, *14*), we sought to identify the main histamine producers in the gut microbiota of patients with IBS. Single bacterial colonies derived from the fecal microbiota of a patient with IBS with high urinary histamine, both before and after transplant into germ-free mice, produced more histamine than did the fecal microbiota of a patient with IBS with low urinary histamine (Fig. 2D). Sanger sequencing identified, at 99% similarity, *K. aerogenes* as the main histamine producer in the fecal microbiota of the patient with IBS with high urinary histamine, whereas *Enterococcus faecium* and *Enterococcus faecalis* were the key histamine-producing bacteria in the fecal microbiota of the patient with IBS with low urinary histamine (table S4). *K. aerogenes* produced 100 times more histamine than any other bacterial isolate ($P = 0.006$ and $P = 0.003$ for anaerobes and aerobes, respectively) (Fig 2D).

We then assessed *K. aerogenes* abundance in the fecal microbiota of patients with IBS and found that it was higher in those with high baseline urinary histamine concentrations but decreased when these patients ate a low fermentable carbohydrate diet (Fig. 2, E and F). The *hdc* gene in Gram-negative bacteria is highly variable (*15*). We identified the *hdc* gene specific for *K. aerogenes* in the stool of 18 of 28 patients with IBS with high urinary histamine, including the patient used in our mechanistic mouse studies. To validate these findings in another IBS patient cohort, we analyzed a recently published dataset from patients with IBS (*16*). We found that compared with healthy controls, patients with IBS had a higher prevalence of *K. aerogenes* spp. and a higher relative abundance of the *hdc* gene ($P = 0.03$ and $P = 0.01$, respectively) (Fig. 2, G and H).

Histamine production by *K. aerogenes MQ* isolate is pH dependent

To compare our *K. aerogenes* McMaster-Queens (*MQ*) isolate with phylogenetically similar strains, we isolated two *Klebsiella oxytoca*

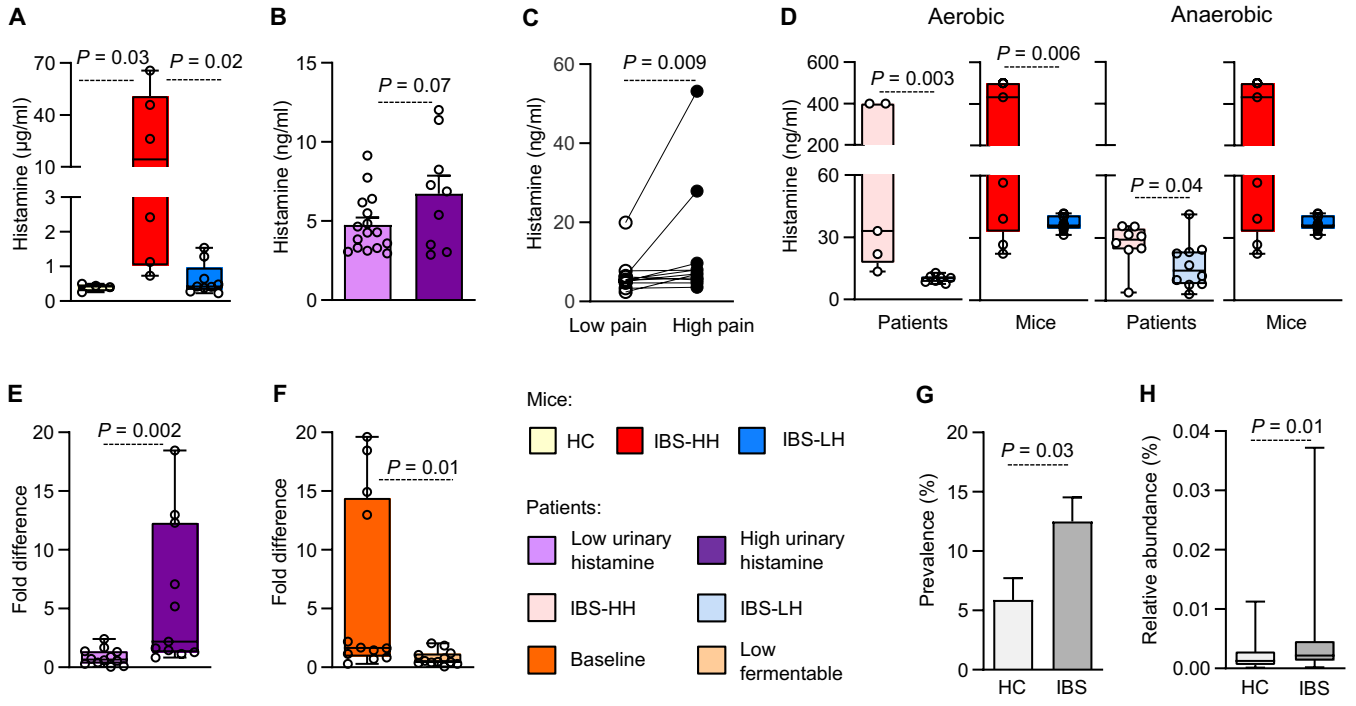

Fig. 2. The gut microbiota of patients with IBS with high urinary histamine produce high amounts of histamine in vitro. (**A**) Histamine production was assessed by ELISA in diluted cecum contents incubated in a semidefined medium containing histidine. Cecum contents were from mice colonized with fecal microbiota from a patient with IBS with high (IBS-HH, red) or low (IBS-LH, blue) urinary histamine or a healthy control (HC, yellow). (**B**) Shown is histamine production in vitro by fecal microbiota from patients with IBS with high or low urinary histamine from our prior clinical study (*2*). The data are shown as means ± SEM. (**C**) Shown is histamine production in vitro by fecal microbiota from patients with IBS in a second longitudinal cohort who experienced low or high abdominal pain. (**D**) Single bacterial colonies were isolated from the stool samples of the two patients used for mechanistic experiments (IBS-HH and IBS-LH) and from mice colonized with fecal microbiota from these two human donors. Single bacterial colonies were cultured in histidine-enriched medium under aerobic or anaerobic conditions, and in vitro production of histamine was assessed by ELISA. (**E**) Shown is the fold difference in *K. aerogenes* relative abundance in the fecal microbiota of patients with IBS with high or low urinary histamine (*2*). The relative abundance of *K. aerogenes* in each sample was calculated with the $2^{\Delta Ct}$ method ($\Delta Ct = Ct$ calibrator $- Ct$ test), where the average *Ct* (cycle threshold) of all samples tested was used as calibrator. (**F**) Shown is the fold difference in *K. aerogenes* relative abundance in the fecal microbiota of patients with IBS before (baseline) and after switching to a low fermentable carbohydrate diet (*2*). (**G**) Shown is the prevalence of *K. aerogenes* in the fecal microbiota of healthy controls (HC) and patients with IBS in a published study (*16*). Data are means ± SEM. (**H**) Shown is the relative abundance of the *hdc* gene in the fecal microbiota of healthy controls (HC) and patients with IBS in a published study (*16*). Unless otherwise stated, the data are shown as medians (minimum – maximum). Data were analyzed using unpaired *t* test (B, D, and G), Mann-Whitney *U* test (E and H), Wilcoxon paired test (C and F), or Kruskal-Wallis test (A) with Dunn's correction.

strains and one *Enterobacter* spp. strain from healthy control individuals. Genomic analysis revealed that *K. oxytoca* strains did not contain the *hdc* gene, as reported previously (*17*), and that both *K. oxytoca* and our *K. aerogenes MQ* isolates had multiple virulence genes (tables S5 and S6). To investigate bacterial histamine production in vivo, we monocolonized germ-free mice with one of these two *Klebsiella* strains. We found that compared with mice colonized with *K. oxytoca* or control germ-free mice, the cecum of mice colonized with the *K. aerogenes MQ* strain had 77 times higher and 145 times higher amounts of histamine, respectively (Fig. 3A).

As bacterial *hdc* activity was previously reported to be pH dependent (*14*), we investigated histamine production by the *K. aerogenes MQ* isolate in different pH environments. Histamine production peaked at pH 7.0 and decreased sharply at pH 6.0 and 8.0 (Fig. 3B), whereas bacterial growth was inhibited only at pH≤5.0 (fig. S4D). This suggested that bacterial histamine production was regulated by the acidity of the colonic milieu, which ranges from pH 5.5 to 7.5 and is modulated by bacterial fermentation (*18*). Lactic acid concentrations (the main determinant of colonic pH) differed greatly between mice colonized with fecal microbiota from patients with IBS with high versus low urinary histamine; this was paralleled by differences in the relative abundance of lactic acid–producing bacteria (Fig. 3, C and D). To investigate whether lactic acid–producing bacteria could regulate histamine production, we cocultured the *K. aerogenes MQ* isolate with a mixture of lactobacilli that decreased histamine production in a concentration-dependent manner (fig. S4D). To confirm this in vivo, we used germ-free mice colonized with a limited gut microbiota (the altered Schaedler flora) consisting of just eight bacterial strains, two of which were lactobacilli (*19*). Mice cocolonized with the *K. aerogenes MQ* isolate or *K. oxytoca* and the lactobacilli had low amounts of histamine and comparable visceral sensitivity (Fig. 3, E to G). This suggested that lactobacilli might modulate histamine production and subsequent visceral hyperalgesia either by lowering the pH and thus decreasing *hdc* activity or less likely by limiting *K. aerogenes MQ* growth (fig. S4F).

Mast cells in the colon may mediate bacterial histamine–induced hyperalgesia

We then investigated the pathways by which bacterial histamine could affect the intestinal neuroimmune system, focusing on mast cells as key intermediaries in nociception (*20*, *21*). First, we performed patch-clamp studies of dorsal root ganglion (DRG) neurons

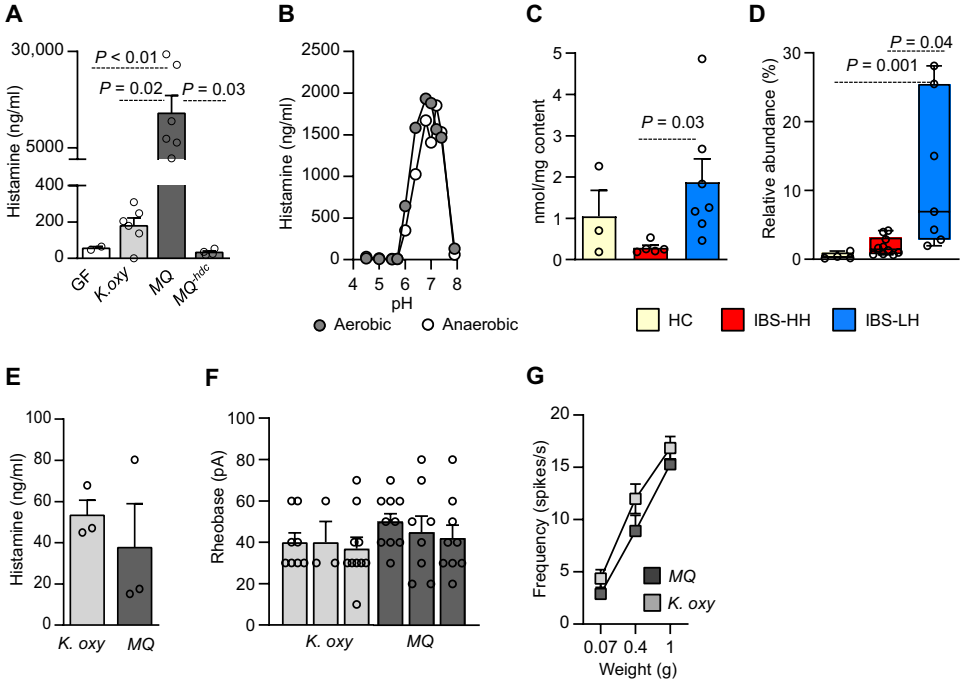

Fig. 3. Bacterial histamine production is modulated by intestinal pH and gut microbial composition. (**A**) Shown is histamine production measured in vitro by ELISA in cultured cecum contents from uncolonized germ-free (GF) mice and germ-free mice monocolonized with different *Klebsiella* isolates. These isolates included *K. oxytoca* (*K. oxy*) from a healthy individual, *K. aerogenes* McMaster-Queens (*MQ*) isolate, and the *MQ* isolate engineered to lack the *hdc* gene (MQ^{-hdc}). Diluted cecum contents were incubated in a semidefined medium containing histidine. (**B**) Shown is histamine production by the *K. aerogenes MQ* isolate cultured in medium with increasing pH under aerobic or anaerobic conditions. (**C**) Lactic acid was measured in the cecum contents of mice colonized with fecal microbiota from a patient with IBS with high (IBS-HH) or low (IBS-LH) urinary histamine or from a healthy control. (**D**) The relative abundance of lactic acid–producing bacteria was assessed in cecum contents from mice colonized with fecal microbiota from a patient with IBS with high (IBS-HH) or low (IBS-LH) urinary histamine or from a healthy control (HC). Data are shown as medians (minimum – maximum). (**E** to **G**) Shown is in vitro histamine production (E), DRG neuronal excitability (rheobase; F), and mechanosensitivity of the colon (G) in ASF mice cocolonized with *K. oxytoca* (*K. oxy*) or *K. aerogenes MQ* isolate. In (F), six naïve SPF mice were used to collect colonic DRG neurons. The DRG neurons were then incubated with colonic supernatants from three ASF mice cocolonized with *K. oxytoca* (light gray bars) or from three ASF mice cocolonized with *K. aerogenes MQ* isolate (dark gray bars). Each circle represents one DRG neuron. In (G), recordings were made from 15 or 16 single afferent units in colons from three mice per group. Unless otherwise stated, the data are shown as means ± SEM. The data were analyzed using unpaired *t* test (E and F), one-way ANOVA (A and C), or two-way ANOVA (G) with Holm-Sidak's correction, or Kruskal-Wallis test (D) with Dunn's correction.

isolated from naïve SPF mice; the neurons were incubated with colonic tissue supernatants from gnotobiotic mice transplanted with the fecal microbiota from human donors. The excitability of these neurons increased (reflected by a decrease in their rheobase) upon incubation with colonic supernatants from mice transplanted with fecal microbiota from patients with IBS ($P = 0.015$ and $P = 0.004$ for a patient with IBS with low or high urinary histamine, respectively) compared with a healthy control microbiota (fig. S5A). This hyperexcitability of DRG neurons was inhibited by the H_1 receptor antagonist pyrilamine and the protease-activated receptor 2 (PAR_2) antagonist GB83 ($P = 0.004$ and $P = 0.015$, respectively) (fig. S5B). GB83 but not pyrilamine inhibited DRG neuron hyperexcitability because of incubation with colonic supernatants from mice colonized with microbiota of the patient with IBS with low urinary histamine ($P = 0.003$) (fig. S5, A and B).

Next, we examined mast cells and their relationship to enteric neurons, because an increased number of colonic mast cells and mast cell colocalization with nerve fibers, together with nerve fiber sprouting, have been described in patients with IBS (*20*–*22*). Mast cells that were immunoreactive for tryptase were increased in the colon of mice colonized with fecal microbiota from patients with IBS with high but not low urinary histamine ($P = 0.03$) (Fig. 4, A and B). Furthermore, many of these mast cells were in close proximity (<2 μm) to PGP9.5-immunoreactive neurons ($P = 0.012$) (Fig. 4, A and B). The colons of mice colonized with fecal microbiota from patients with IBS also had a higher density of neurons compared with the colons of mice colonized with a healthy control fecal microbiota (fig. S5C). To investigate whether the *K. aerogenes MQ* isolate could induce a similar increase in colonic mast cell number, we assessed colon tissues from monocolonization experiments where germ-free mice were gavaged with only one bacterial strain. Mice colonized with the *K. aerogenes MQ* isolate had increased mast cells compared with mice colonized with *K. oxytoca* or germ-free mice ($P = 0.01$ and $P < 0.001$, respectively) (Fig. 4C). However, mast cell numbers remained low in ASF mice cocolonized with the *K. aerogenes MQ* isolate or *K. oxytoca* (Fig. 4D).

Bacterial histamine acts a chemoattractant for colonic mast cells

Given that histamine is known to enhance mast cell migration and recruitment to tissues (*23*), we set out to confirm that the increased mast cell numbers observed in mice monocolonized with the *K. aerogenes MQ* isolate was due to bacterial histamine production. We created a new *Klebsiella* strain MQ^{-hdc} by deleting the *hdc* gene from the *MQ* isolate (fig. S4G). We used this strain to monocolonize another group of germ-free mice. Colons from mice monocolonized with the MQ^{-hdc} strain had lower numbers of mast cells than did colons from mice monocolonized with the wild-type *MQ* strain ($P = 0.001$) (Fig. 4C); the former mouse group had negligible amounts of histamine in cecum contents compared with the latter mouse group (Fig. 3E). Conversely, colons from germ-free mice monocolonized with a laboratory strain of *Escherichia coli* engineered to express the *hdc* gene ($E. coli^{hdc}$) showed increased histamine production and mast cell numbers compared with colons from mice monocolonized with the original *E. coli* strain (fig. S4, G and H). $E. coli^{hdc}$ monocolonization resulted in lower histamine production and smaller colonic mast cell numbers than did monocolonization with the *K. aerogenes MQ* isolate. Presumably, this occurs because $E. coli^{hdc}$ lacks the specific gene encoding the histidine/histamine antiporter, which is mainly responsible for histamine transport from the cell to the environment.

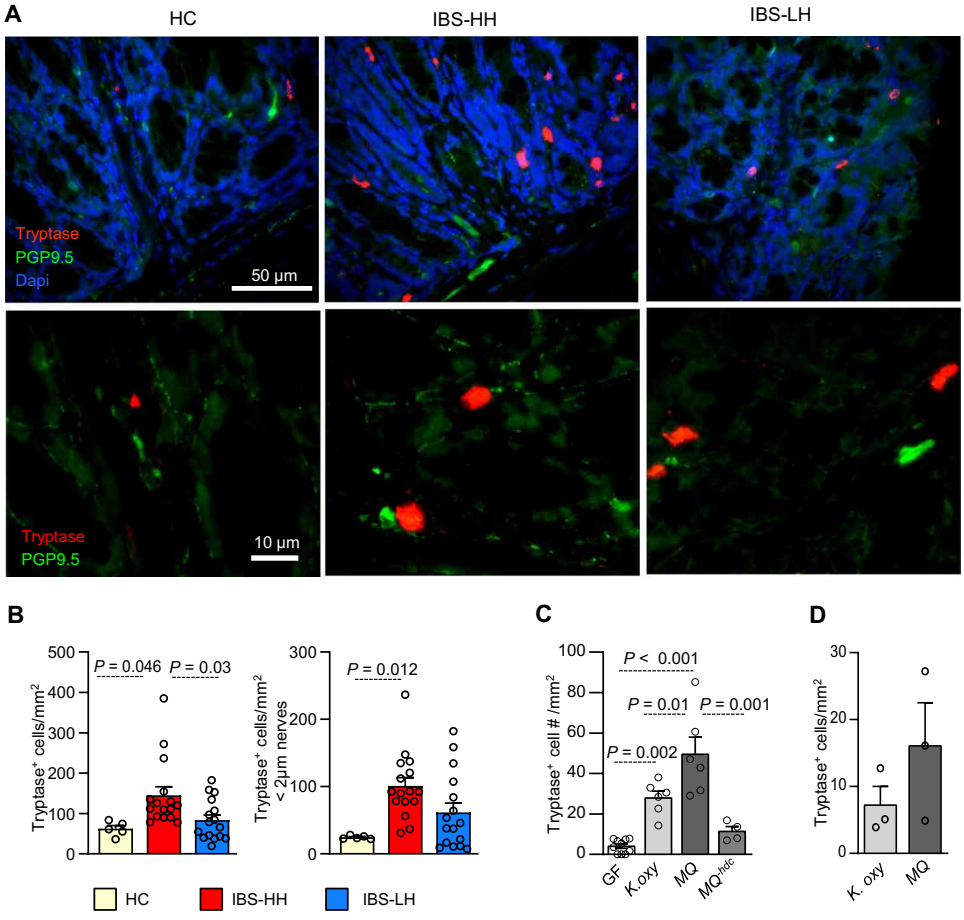

Fig. 4. Effects of histamine-producing bacteria on mast cells and mast cell–nerve interactions. (**A**) Shown are representative images of immunofluorescence staining in colon tissue from germ-free mice colonized with fecal microbiota from a patient with IBS with high (IBS-HH) or low (IBS-LH) urinary histamine or from a healthy control. Images show tryptase staining (red) for colonic mast cells and PGP9.5 staining (green) for colonic neurons. (**B**) Shown is the total number of mast cells (tryptase positive) and the number of mast cells localized within 2 µm of neurons in the colons of mice colonized with fecal microbiota from a patient with IBS with high (IBS-HH) or low (IBS-LH) urinary histamine or from a healthy control (HC). (**C**) Shown is the total number of mast cells (tryptase positive) in colons of germ-free (GF) mice or germ-free mice monocolonized with *K. oxytoca* (*K. oxy*) isolated from a healthy individual, *K. aerogenes MQ* isolate, or *K. aerogenes MQ* isolate engineered to lack the *hdc* gene (MQ^{-hdc}). (**D**) Shown is the total number of mast cells (tryptase positive) in colons of ASF mice cocolonized with *K. oxytoca* (*K. oxy*) or *K. aerogenes MQ* isolate (MQ). Unless otherwise stated, the data are shown as means ± SEM. The data were analyzed using a one-way ANOVA (B and C) with Holm-Sidak's correction or unpaired *t* test (D). Each experiment was performed on 3 to 16 mice.

Bacterial histamine–induced visceral hyperalgesia is mediated by H4 receptor signaling

To gain insight into the specific pathways by which bacterial histamine could affect the gut neuroimmune system, we studied known chemoattractants and activators of mast cells, CXCL12 and interleukin-33 (IL-33), as well as the mast cell–nerve interaction modulator VIP_1R (*23*, *24*). Colons from germ-free mice colonized with IBS fecal microbiota showed higher CXCL12, IL-33, and VIP_1R expression compared with colons from mice colonized with a healthy fecal microbiota. There was, however, no difference in CXCL12, IL-33, and VIP_1R expression between mice colonized with fecal microbiota from patients with IBS with high versus low urinary histamine (fig. S5, D to F). Furthermore, colonic H_1 and H_2 receptor expression was similar among all germ-free mice colonized with IBS or healthy control microbiota (fig. S5, G and H). The H_4 receptor (H_4R) has been implicated in colitis (*25*, *26*) and visceral hypersensitivity (*25*–*27*), so we explored whether it could be mediating the effects of bacterial histamine. Histamine has a greater affinity for H_4R than H_1 and H_2 receptors, and H_4R signaling has been proposed to mediate mast cell migration and recruitment (*23*). We found that H_4R expression was upregulated in the colons of mice colonized with fecal microbiota from patients with IBS with high urinary histamine (Fig. 5, A and B). H_4R was expressed in colonic epithelial cells, mast cells, goblet cells, intraepithelial lymphocytes, macrophages, and enteroendocrine cells (Fig. 5C). We hypothesized that bacterial histamine may induce mast cell migration and activation through H_4R signaling, leading to visceral hyperalgesia. Therefore, we incubated bone marrow–derived mast cells with cell-free supernatants of cecal contents from mice colonized with healthy control or IBS fecal microbiota. Cell-free cecal contents from mice colonized with fecal microbiota from a patient with IBS with high urinary histamine induced increased chemotaxis of bone marrow–derived mast cells ($P = 0.02$) (Fig. 5D), which was blocked by the H_4R antagonist JNJ-7777120 ($P < 0.001$) (Fig. 5D). We then colonized a new group of germ-free mice with fecal microbiota from a patient with IBS with high urinary histamine and administered the mice a different H_4R antagonist, JNJ-39758979, or placebo for 3 weeks. Compared with placebo, JNJ-39758979 treatment reduced in vivo visceromotor responses to colorectal distension ($P = 0.021$ and $P = 0.011$ for 100 and 200 µl of colorectal distension, respectively), in vitro firing of colonic afferent nerves ($P < 0.001$), and decreased colonic mast cell numbers ($P = 0.046$) (Fig. 5, E to G). Furthermore, the excitability of DRG neurons isolated from naïve SPF mice and incubated with colonic supernatants from mice colonized with fecal microbiota from a patient with IBS with high urinary histamine was reduced if the mice had been treated with JNJ-39758979 compared with placebo ($P = 0.037$) (Fig. 5H).

DISCUSSION

It is well established that intestinal immune activation leads to peripheral sensitization and hyperalgesia (*21*, *22*), but the triggers of this activation are largely unknown. Clinical studies suggest that mast cells are involved in visceral pain in patients with IBS as indicated by hyperplasia and activation of mast cells and their proximity to nerve terminals in colonic tissues from patients with IBS, and

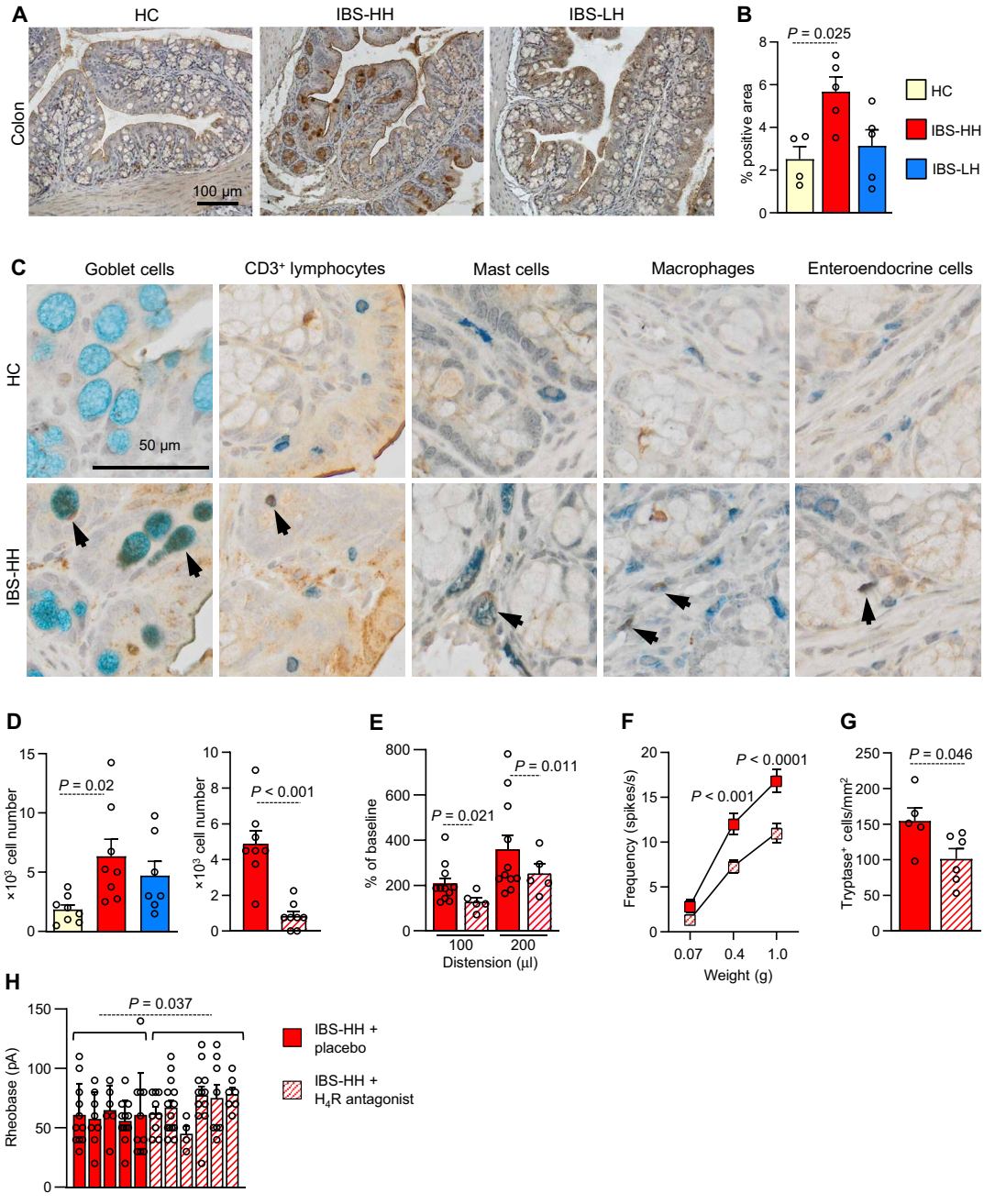

Fig. 5. H_4R mediates the effects of histamine produced by gut microbiota. (**A**) Shown are representative images of H_4R immunoreactivity (brown) in colon tissues from mice colonized with fecal microbiota from a patient with IBS with high (IBS-HH) or low (IBS-LH) urinary histamine or from a healthy control (HC). (**B**) Quantification of H_4R immunoreactivity in colon tissues from mice colonized with fecal microbiota from a patient with IBS with high (IBS-HH) or low (IBS-LH) urinary histamine or from a healthy control (HC). The data are shown as means ± SEM. (**C**) Shown are representative images of H_4R immunoreactivity (brown) colocalized (black arrow) with markers for other cells (blue) in colon tissues from mice colonized with fecal microbiota from a patient with IBS with high (IBS-HH) or low (IBS-LH) urinary histamine or from a healthy control (HC). (**D**) Left: Shown is the number of migrating cells among cultured bone marrow–derived mast cells after incubation with cell-free supernatants of cecal contents from germ-free mice colonized with fecal microbiota from a patient with IBS with high (IBS-HH, red) or low (IBS-LH, blue) urinary histamine or from a healthy control (yellow). Right: Shown is the number of migrating cells among cultured bone marrow–derived mast cells incubated with cell-free supernatants of cecal contents from germ-free mice colonized with fecal microbiota from a patient with IBS with high urinary histamine (IBS-HH) and treated with placebo (red) or the H_4R antagonist JNJ-7777120 (red stripes). The data are shown as means ± SEM. (**E** to **G**) Shown are visceromotor responses to colon distension, colon mechanosensitivity measured with the vFH test, and mast cell numbers in colon tissue from mice colonized with fecal microbiota from a patient with IBS with high urinary histamine (IBS-HH) after treatment with placebo (red) or the H_4R antagonist JNJ-39758979 (red stripes). (**H**) Shown is excitability (rheobase) of DRG neurons (isolated from five naïve SPF mice) incubated with colonic supernatants from germ-free mice colonized with fecal microbiota from a patient with IBS with high urinary histamine (IBS-HH) and treated with placebo (red) or the H_4R antagonist JNJ-39758979 (red stripes). Each circle represents one DRG neuron. The data were analyzed with one-way ANOVA (B and D, left), two-way ANOVA (F) with Holm-Sidak's correction, or an unpaired *t* test (D, right; E; G; and H). Each experiment was performed on 4 to 12 mice.

their positive correlation with pain scores (*22*). We have previously shown that reducing dietary content of fermentable carbohydrates leads to a decrease in abdominal pain in a subset of patients with IBS, which is accompanied by changes to the gut microbiota and a decrease in urinary histamine (*2*). In the current study, we used a diet high in fermentable carbohydrates to elicit similar visceral hypersensitivity in germ-free mice colonized with the fecal microbiota of patients with IBS with high urinary histamine. We demonstrated that mechanisms underlying visceral hypersensitivity are dependent on the individual microbial community and its metabolic activity. We show that bowel distension alone due to bacterial fermentation is unlikely to account for the visceral hyperalgesia observed in the gnotobiotic mice. This is in line with previous reports (*28*) suggesting that visceral hypersensitivity in response to abdominal

distension rather than gas production itself triggers symptoms in patients with IBS eating a high fermentable carbohydrate diet (*29*).

In patients with IBS, activation of mast cells and their close proximity to nerve terminals (*22*), together with colonic intraluminal proteases (*30*, *31*), participate in sensitization of sensory nerves leading to abdominal pain. Here, we demonstrate that microbially derived histamine can trigger mast cell activation. We show that germ-free mice colonized with the fecal microbiota of patients with IBS with high urinary histamine produced high amounts of histamine, resulting in visceral hypersensitivity, increased nerve density, and up-regulation of genes involved in mast cell activation in the colon.

Although, traditionally, mast cells have been considered to be the main source of histamine, our findings point to the gut microbiota as an important source. We identified a specific bacterium, *K. aerogenes* spp., which produced high amounts of histamine. Furthermore, we provided direct evidence that bacterial histamine produced by *K. aerogenes* led to visceral hyperalgesia mediated by H_4 receptor–dependent signaling that has previously been implicated in both mast cell recruitment (*23*) and visceral sensitivity (*25*–*27*). We demonstrated that *K. aerogenes* was present in the gut microbiota of patients with IBS with high urinary histamine and decreased with a low fermentable carbohydrate diet in parallel with a decrease in abdominal pain. We also showed that pain severity correlated with microbial histamine production in patients with IBS followed longitudinally.

Our study has several limitations. First, a direct effect of bacterial histamine on sensory nerves was not demonstrated, and further studies are needed to assess the contribution of histamine to visceral hyperalgesia. Second, the involvement of a PAR_2 pathway in the increased excitability observed in DRG neurons incubated with colon supernatants from mice colonized with fecal microbiota from patients with IBS was shown in vitro but was not further investigated in vivo. Whereas bacterial histamine may be a key driver of abdominal pain in one-third of patients with IBS, bacterial proteases are likely to be involved in nociception in other patient subgroups, and this should be explored in future studies. Third, additional experiments are needed to support our observations of the role of lactobacilli and the ASF microbiota on microbial histamine modulation, because our initial studies used a limited number of mice and did not directly assess visceral sensitivity.

In conclusion, our study establishes that visceral hypersensitivity can be shaped by an individual's gut microbial community, through a specific diet-microbial interaction involving histamine production. Our results provide evidence that bacterial histamine may lead to intestinal mast cell hyperplasia and activation through an H_4 receptor–dependent pathway, triggering visceral hyperalgesia. In agreement with clinical trial data, our findings suggest that gas production with bowel distension is not the primary nociceptive trigger in patients with IBS consuming a high fermentable diet and may help to explain why only some patients respond clinically to a low fermentable diet (*28*, *32*). Identifying those patients will be crucial as the low microbial diversity in Western populations, which has been linked to many chronic diseases, can further decrease when restriction of dietary fiber is recommended (*33*). The identification of *K. aerogenes*, or bacteria with similar *hdc* activity, as a source of histamine in the gut may guide dietary recommendations, microbiota-directed therapies, or use of H_4 receptor antagonists in a subset of patients with IBS with chronic abdominal pain.

MATERIALS AND METHODS

Study design

The objective of our study was to investigate whether the gut microbiota can induce visceral hypersensitivity through histamine production. First, data from our prior clinical study in patients with IBS investigating the effect of a high or low fermentable diet (*2*) were reanalyzed to examine the relationship between abdominal pain and urinary histamine concentrations. We then selected 10 patients with IBS from that study (*2*), with either high urinary histamine ($n = 5$) or low urinary histamine ($n = 5$) (table S1). We used their stool samples obtained at baseline (before dietary intervention) to colonize germ-free mice for initial experiments investigating visceral sensitivity. From those patients with IBS, one patient with high urinary histamine (0.340 ng/ml) and one with low urinary histamine (0.014 ng/ml) were selected as fecal microbiota donors for subsequent mechanistic studies. A stool sample from a healthy volunteer (sex and age matched, with no gastrointestinal symptoms) was used to colonize germ-free mice in the control group. Another cohort of patients with IBS ($n = 11$) that was followed longitudinally for 6 months at McMaster University Medical Center was included to study the relationship between stool histamine abundance and pain scores. Their symptoms were monitored, and stool samples were collected on a weekly basis (table S5). The study was approved by the Hamilton Integrated Research Ethics Boards (HiREB #11-445) at McMaster University. All participants signed the informed consent form before enrollment.

Animals

Germ-free National Institutes of Health (NIH) Swiss and C57BL/6 mice (8 to 10 weeks old) were provided by the Axenic Gnotobiotic Unit of McMaster University. The mice were gavaged with either diluted human fecal samples (1:10 in saline) or fresh pure bacterial cultures and housed for 3 weeks in sterilized individually ventilated racks, on a 12-hour light/12-hour dark cycle with free access to food and water, as previously described (*8*). SPF mice were bred in the McMaster University Central Animal Facility. All experiments were approved by the McMaster University Animal Care Committee and Queen's University Animal Care Committee.

Germ-free NIH Swiss mice ($n = 120$) were colonized with fecal microbiota samples from patients with IBS or a healthy volunteer and kept in ISOcages (Techniplast). Germ-free mice were switched from a regular mouse chow to a custom-made diet containing high or low amounts of fermentable carbohydrates (table S2) 3 days before transplantation with human fecal microbiota and were maintained on these diets during the entire duration of the experiments. Mice of both sexes were randomly selected for bacterial colonization, and each group was evenly balanced for female:male ratio. Three weeks after colonization, we collected fecal samples and performed CT imaging.

After euthanizing the mice, ex vivo recordings were performed from single axons in nerve bundles innervating the distal colon (*34*), and patch-clamp recordings were performed from DRG neurons incubated overnight with colonic tissue supernatants (*35*, *36*). A control group of mice harboring SPF microbiota ($n = 18$), the normal mouse microbiota, also followed the same protocol.

To assess the role of H_4R, an additional group of germ-free mice ($n = 33$) were colonized with the fecal microbiota of one patient with IBS with high urinary histamine and fed the custom-made diet with high fermentable carbohydrates. Starting the day of the colonization,

the H_4R antagonist JNJ-39758979A was administered in drinking water to 18 mice for 3 weeks using previously established protocols and dosing (50 mg/kg per day) (*37*–*39*); the other 15 control mice continued to drink water only. Water consumption was monitored daily; the water with the H_4R antagonist was changed daily until the mice were euthanized.

Germ-free C57BL/6 mice (n = 22) were also monocolonized by receiving one oral gavage with either 10^9 colony-forming units (CFUs) of either *MQ K. aerogenes* isolate (n = 6 mice), *K. oxytoca* (isolated from a healthy control) (n = 6), MQ^{-hdc} isolate (MQ strain lacking the *hdc* gene) (n = 4), *E. coli* as a control (n = 3), or recombinant $E.\ coli^{hdc}$ (n = 3). Mice were kept in ISOcages (Techniplast) within the axenic gnotobiotic unit until euthanasia. The investigators were blinded to group allocation for all the assessments, except for gene expression analysis.

Fecal microbiota analysis

Stool samples were collected 3 weeks after colonization and immediately frozen at −80°C. Colonic and cecal content samples were collected at euthanasia. Total genomic DNA was extracted from the stool samples as previously described (*40*). After this protocol, amplification of the V3 region of the 16*S* rRNA gene and Illumina sequencing were performed as previously described (*40*, *41*). Briefly, the data were analyzed following the pipelines of dada2 (*42*) and QIIME2 (*43*). Taxonomic assignments were performed using the Ribosomal Database Project (RDP) classifier (*44*) with the Greengenes (*45*) training set. Analyses were done using either QIIME2 (*43*), MaAsLin (*46*), PICRUSt (*47*), phyloseq package (1.28) (*48*) for R (3.6.1), or SPSS software v. 23. All results were corrected for multiple comparisons, allowing a 5% false discovery rate.

Bacterial histamine production in vitro

Mouse cecal samples or human fecal samples were diluted 1:10 (weight: volume) with sterile phosphate-buffered saline, and 10 µl was inoculated into 5 ml of semidefined medium, LDMIII (*49*), with or without L-histidine (4 g/liter) (Sigma-Aldrich Canada Co., Oakville, Canada). After 20 hours, cultures were centrifuged, and supernatants were collected, sterilized with 0.22-µm-sized syringe filters (Millipore, Etobicoke, Canada), and stored at −80°C until analysis. Pellets were stored at −80°C in 20% skim milk (1:1). The stored pellets were then plated on generic solid media, such as brain heart infusion (BHI), de Man, Rogosa, and Sharpe (MRS), and MacConkey (Oxoid, Canada) and incubated in anaerobic and aerobic conditions. In total, 164 colonies were picked and tested in vitro for their capacity to produce histamine from histidine, as was done for cecal and fecal samples above. The DNA of each bacterial strain that produced histamine was extracted, and the 16*S* rRNA gene was amplified with the following primers: 8F, 5′-AGAGTTTGATCCTGGCTCAG-3′; 926R, 5′-CCGTCAATTCCTTTRAGTTT-3′. The resulting amplicon was sent for Sanger sequencing for identification purposes (GENEWIZ Services, NJ, USA). Cocultures of *MQ K. aerogenes* isolate and a lactobacilli mixture were performed as described for single colonies. Both strains were seeded at 10^8 CFU/ml. The supernatants were collected after 20 hours, and histamine was measured by enzyme-linked immunosorbent assay (ELISA). pH studies were performed using a regrowth of the original colony of *MQ* isolate at a concentration of 10^8 CFU/ml. For the kinetics, 2 µl of *MQ* was added to 198 µl of LDMIII (*49*) in triplicate in a sterile tissue culture 96-well plate. The plate was then incubated aerobically at 37°C for 20 hours (two reads per hour). The pH of LDMIII was modified with varying concentrations of citric acid–sodium citrate buffer (pH 4 to 6) and Na_2HPO_4-NaH_2PO_4 buffers (pH6 to 8). An additional identical plate was incubated anaerobically. The supernatants were collected after 20 hours, and histamine was measured by ELISA at end point.

K. aerogenes qPCR and hdc gene detection

K. aerogenes and *hdc* gene relative quantification was performed on the genomic DNA by quantitative real-time polymerase chain reaction (PCR) on the CFX Connect Real-Time System (Bio-Rad and Applied Biosystems) using the following custom in-house–designed primers for *hdc* gene of Gram-negative bacteria, *hdc*1f: 5′-GCCATCCCATCATTTTCGCC-3′ and hdc1r: 5′- CCGGAAACGCCAATCGAATC-3′, generating a product size of 214 base pairs (bp) and with a T_m of 60°C. For *K. aerogenes*, the following primers were used: KA-F 5′-GTAACCGGTGAAACCGAAAGC-3′ and KA-R 5′-GATGCCGCCTTCGTAGTGGAAATGG-3′ (reverse), generating a product size of 201 bp and with a T_m of 60°C. The PCR mix contained 1 µl of 50 ng/µl of fecal genomic DNA, 7 µl of ultrapure water, 1 µl of each primer, and 10 µl of SsoFast EvaGreen Supermix (Bio-Rad and Applied Biosystems, Mississauga, ON, Canada). Multiple negative and positive controls were included in all plates, as well as a calibration curve, to ensure optimal PCR efficiency. The data were expressed as the expression of *K. aerogenes* or *hdc* in each sample relative to the rest of the samples: $2^{\Delta Ct}$, where $\Delta Ct = Ct$ calibrator − Ct test. The average of the Ct of all samples tested was used as calibrator.

Data mining

The published dataset from Mars and colleagues (*16*) was analyzed for the presence and abundance of histamine-producing bacteria, according to the presence of *hdc* gene [Kyoto Encyclopedia of Genes and Genomes (KEGG) ortholog K01590, EC:4.1.1.22] in the metagenomic data. A list of bacteria harboring the enzyme was downloaded from the KEGG, and all the species found in the dataset were analyzed for differential prevalence and abundance between healthy controls and patients with IBS at baseline. The *hdc* gene was found in all individuals, but the relative abundance was higher in patients with IBS at baseline.

Histamine measurement by ELISA

Histamine was measured with the Histamine ELISA Kit (Enzo, Cedarlane Laboratories, Burlington, ON, Canada) according to the manufacturer's instructions.

Visceromotor responses to colorectal distension

Mice were briefly anesthetized with isoflurane 3% (Isoflurane USP 99.9%, Fresenius Kabi, Toronto, Canada), and a custom-made catheter balloon (20 mm long by 10 mm wide) was delicately inserted into the colon of mice with the distal end positioned 5 mm proximally from the anus, as previously described (*50*). Mice were then placed in a custom-made harness containing two EMG electrodes (sterile 30-gauge needles, Becton Dickinson, Mississauga, Canada) penetrating the mid abdominal muscle at a depth of 1 mm and a ground electrode clipped on the mouse tail. Mice were then suspended in a rodent sling (Lomir Biomedical, Notre Dame de-l'île-Perrot, Canada), and the electrodes and balloon catheter were connected to a custom-made barostat. After 5 min of rest, the balloon was inflated for 10 s, (volume, 100 and 200 µl), in triplicate, with resting

intervals of 4 min between consecutive distensions. Each distension period consisted of 7-s baseline activity, 10-s stimulation, and 3-s postdistension. Abdominal muscle EMG activity was recorded using customized software (Labview Express 7).

Ex vivo extracellular recordings from mouse colon

After the mice were euthanized, the colon (5 to 6 cm) and attached mesentery (containing the lumbar colonic nerves) were removed intact, along with the attached neurovascular bundle as described previously (*34*). Briefly, the distal colon was carefully opened along the mesenteric border, with care taken not to damage the mesenteric nerves, and placed in a specialized organ bath. Preparations were superfused with a modified Krebs' solution containing the following: 118.4 mM NaCl, 24.9 mM $NaHCO_3$, 1.2 mM KH_2PO_4, 1.2 mM $MgSO_4(H_2O)_7$, 1.9 mM $CaCl_2$, and 11.7 mM D-glucose, bubbled with carbogen (95% O_2/5% CO_2) at a temperature of 33° to 34°C. All preparations contained nifedipine (3 μM) and atropine (5 μM) to suppress smooth muscle activity and the prostaglandin synthesis inhibitor indomethacin (3 μM) to suppress potential inhibitory actions of endogenous prostaglandins (*51*). Using fine forceps, the nerve trunk was teased apart into four to six bundles, one of which was drawn into a borosilicate glass suction electrode (World Precision Instruments) prefilled with Krebs buffer. Electrical signals generated by nerve bundles were amplified, filtered, and sampled at a rate of 10 kHz, using a 1401 interface (Cambridge Electronic Design). Action potentials were analyzed off-line using the Spike 2 wave mark function and discriminated as single units on the basis of distinguishable waveform and amplitude. Mechanosensitivity was assessed in single axons, classified as either serosal or mesenteric (*34*), which collectively have been characterized as vascular afferents (*52*); these axons only responded to probing with a 1-g von Frey hair (vFH) with no response to circumferential stretch (5 g for 1 min) or light mucosal stroking. Once identified, mechanical stimulation by vFH (0.07 to1 g) was applied to the receptive field four times, each for 3 s, and the average of the largest three responses was calculated.

DRG dissection and culture

DRG neurons (T9 to T13) were acutely dissociated as previously described (*53*, *54*). Dispersed neurons were suspended in F12 medium (Sigma-Aldrich, St. Louis, Missouri, USA) pH 7.2 to 7.3, 10% fecal calf serum, plated on laminin/poly-D-lysine–coated (60 μl /ml) coverslips (Inamed Biomaterials, Fremont, CA, USA) and incubated at 95% O_2 and 5% CO_2. Two hours after plating, cells were incubated with the supernatant/F12 medium (50 μl of supernatant combined with 950 μl of F12 medium) and incubated overnight (18 to 24 hours) until retrieval for electrophysiological studies.

Immunofluorescence and immunohistochemistry

Tissues were fixed overnight in 10% formalin and paraffin embedded. Four-micrometer paraffin sections were mounted on coated slides, dewaxed, and rehydrated. Tryptase (1:200; ab151757, Abcam, ON, Canada) and PGP9.5 (1:250; ab10410, Abcam) immunofluorescence was performed on formalin-fixed mouse colon tissue sections. Briefly, after deparaffinization, antigen retrieval process with a citric acid buffer, and saturation of nonspecific sites with BSA (5%, 30 min), sections were incubated with primary antibodies overnight in a humidified chamber at 4°C. Conjugated secondary antibodies, Alexa Fluor 555–conjugated donkey anti-rabbit (A-31572, Invitrogen), Alexa Fluor 488–conjugated donkey anti–guinea pig (706-545-148, Jackson ImmunoResearch Inc., PA, USA), and Alexa Fluor-647–conjugated chicken anti-rat (A-21472, Invitrogen) were used. Slides were mounted in ProLong Gold with 4′,6-diamidino-2-phenylindole (DAPI) (ProLong Gold antifade regent with DAPI, Thermo Fisher Scientific, ON, Canada). Pictures were taken using an epifluorescence microscope (Eclipse 80, Nikon, ON, Canada) with the same setting and exposure time for all pictures. For each section, 11 to 13 micrographs were taken from mucosa and submucosa. The quantification was performed with NIS-Element Basic Research B12 Analysis (Nikon) by counting tryptase immunoreactive (positive) cells, tryptase immunoreactive (positive) cells within 2 μm of PGP9.5 immunoreactive (positive) cells, tryptase immunoreactive (positive) area, and PGP9.5 immunoreactive (positive) area (power field: 40× objective lens).

Immunohistochemistry was performed to characterize the expression of H_1R (TA 317909, OriGene, Rockville, MD), H_2R (TA340793, OriGene), and H_4R (TA340671, OriGene) in mouse colon tissues. ImmPRESS polymer reagent anti-goat or anti-rabbit (Vector Laboratories, Burlingame, CA) and ImmPACT DAB (3, 3 -diaminobenzidine) peroxidase substrate (Vector Laboratories) were used for detection. The sections were stained with Gill's hematoxylin as a counterstain. Images were captured by an automatic slide scanner microscope (Olympus VS 120-S6-W, Olympus, Richmond Hill, ON, Canada). This automatic slide scanner can digitalize whole slides at ×20 magnifications. Quantification was performed with ImageJ software (NIH, Bethesda, MD). H_4R was costained with Alcian blue to reveal goblet cells, CD3 (ab11089, Abcam), tryptase (MA5-11711, Invitrogen), CD11b (14-0112-82, Invitrogen), and chromogranin A (ab715, Abcam). CD3, tryptase, CD11b, and chromogranin A were detected by VECTASTAIN ABC-AP and Vector Blue Alkaline Phosphatase Substrate (Vector Laboratories). For tryptase and chromogranin A staining, the tissues were treated with M.O.M Mouse Immunoglobulin G (IgG) Blocking Reagent and M.O.M. Biotinylated Anti-Mouse IgG Reagent (Vector Laboratories). The images were captured by a Nikon microscope (Eclipse 80, Nikon, ON, Canada) with ×40 magnification.

Statistical analysis

Statistical analyses were performed using SPSS 23.0 software for Windows (SPSS Inc., Chicago, IL, USA), R (version 3.6.0), and GraphPad Prism. The data are presented as median Interquartile Deviation (IQD) or means ± SEM. Statistical comparisons were performed using two-way analysis of variance (ANOVA), one-way ANOVA, *t* test, Mann-Whitney, or Kruskal-Wallis test. Benjamini and Hochberg false discovery rate, Tukey, Dunn's, or Holm-Sidak's correction method was used when multiple comparisons were performed. $P < 0.05$ was considered statistically significant.

SUPPLEMENTARY MATERIALS

www.science.org/doi/10.1126/scitranslmed.abj1895
Methods
Figs. S1 to S5
Tables S1 to S6
Data file S1
MDAR Reproducibility Checklist
References (*55*–*75*)

View/request a protocol for this paper from *Bio-protocol*.

REFERENCES AND NOTES

1. A. H. Keshteli, K. L. Madsen, R. Mandal, G. E. Boeckxstaens, P. Bercik, G. De Palma, D. E. Reed, D. Wishart, S. Vanner, L. A. Dieleman, Comparison of the metabolomic profiles

of irritable bowel syndrome patients with ulcerative colitis patients and healthy controls: New insights into pathophysiology and potential biomarkers. *Aliment. Pharmacol. Ther.* **49**, 723–732 (2019).
2. K. McIntosh, D. E. Reed, T. Schneider, F. Dang, A. H. Keshteli, G. De Palma, K. Madsen, P. Bercik, S. Vanner, FODMAPs alter symptoms and the metabolome of patients with IBS: A randomised controlled trial. *Gut* **66**, 1241–1251 (2017).
3. A. Minerbi, E. Gonzalez, N. J. B. Brereton, A. Anjarkouchian, K. Dewar, M. A. Fitzcharles, S. Chevalier, Y. Shir, Altered microbiome composition in individuals with fibromyalgia. *Pain* **160**, 2589–2602 (2019).
4. M. Lyte, Microbial endocrinology: Host-microbiota neuroendocrine interactions influencing brain and behavior. *Gut Microbes* **5**, 381–389 (2014).
5. N. Cenac, C. N. Andrews, M. Holzhausen, K. Chapman, G. Cottrell, P. Andrade-Gordon, M. Steinhoff, G. Barbara, P. Beck, N. W. Bunnett, K. A. Sharkey, J. G. Ferraz, E. Shaffer, N. Vergnolle, Role for protease activity in visceral pain in irritable bowel syndrome. *J. Clin. Invest.* **117**, 636–647 (2007).
6. A. Olivera, M. A. Beaven, D. D. Metcalfe, Mast cells signal their importance in health and disease. *J. Allergy Clin. Immunol.* **142**, 381–393 (2018).
7. G. E. Boeckxstaens, M. M. Wouters, Neuroimmune factors in functional gastrointestinal disorders: A focus on irritable bowel syndrome. *Neurogastroenterol. Motil.* **29**, e13007 (2017).
8. G. De Palma, M. D. Lynch, J. Lu, V. T. Dang, Y. Deng, J. Jury, G. Umeh, P. M. Miranda, M. Pigrau Pastor, S. Sidani, M. I. Pinto-Sanchez, V. Philip, P. G. McLean, M. G. Hagelsieb, M. G. Surette, G. E. Bergonzelli, E. F. Verdu, P. Britz-McKibbin, J. D. Neufeld, S. M. Collins, P. Bercik, Transplantation of fecal microbiota from patients with irritable bowel syndrome alters gut function and behavior in recipient mice. *Sci. Transl. Med.* **9**, (2017).
9. S. J. Shepherd, F. C. Parker, J. G. Muir, P. R. Gibson, Dietary triggers of abdominal symptoms in patients with irritable bowel syndrome: Randomized placebo-controlled evidence. *Clin. Gastroenterol. Hepatol.* **6**, 765–771 (2008).
10. C. J. Tuck, S. J. Vanner, Dietary therapies for functional bowel symptoms: Recent advances, challenges, and future directions. *Neurogastroenterol. Motil.* **30**, e13238 (2017).
11. A. Koh, F. De Vadder, P. Kovatcheva-Datchary, F. Backhed, From dietary fiber to host physiology: Short-chain fatty acids as key bacterial metabolites. *Cell* **165**, 1332–1345 (2016).
12. R. Soret, J. Chevalier, P. De Coppet, G. Poupeau, P. Derkinderen, J. P. Segain, M. Neunlist, Short-chain fatty acids regulate the enteric neurons and control gastrointestinal motility in rats. *Gastroenterology* **138**, 1772–1782.e4 (2010).
13. M. Schirone, P. Visciano, R. Tofalo, G. Suzzi, Histamine food poisoning. *Handb. Exp. Pharmacol.* **241**, 217–235 (2017).
14. J. M. Landete, B. D. l. Rivas, A. Marcobal, R. Munoz, Updated molecular knowledge about histamine biosynthesis by bacteria. *Crit. Rev. Food Sci. Nutr.* **48**, 697–714 (2008).
15. H. Takahashi, B. Kimura, M. Yoshikawa, T. Fujii, Cloning and sequencing of the histidine decarboxylase genes of Gram-negative, histamine-producing bacteria and their application in detection and identification of these organisms in fish. *Appl. Environ. Microbiol.* **69**, 2568–2579 (2003).
16. R. A. T. Mars, Y. Yang, T. Ward, M. Houtti, S. Priya, H. R. Lekatz, X. Tang, Z. Sun, K. R. Kalari, T. Korem, Y. Bhattarai, T. Zheng, N. Bar, G. Frost, A. J. Johnson, W. van Treuren, S. Han, T. Ordog, M. Grover, J. Sonnenburg, M. D'Amato, M. Camilleri, E. Elinav, E. Segal, R. Blekhman, G. Farrugia, J. R. Swann, D. Knights, P. C. Kashyap, Longitudinal multi-omics reveals subset-specific mechanisms underlying irritable bowel syndrome. *Cell* **182**, 1460–1473.e17 (2020).
17. M. Kanki, T. Yoda, T. Tsukamoto, T. Shibata, *Klebsiella pneumoniae* produces no histamine: *Raoultella planticola* and *Raoultella ornithinolytica* strains are histamine producers. *Appl. Environ. Microbiol.* **68**, 3462–3466 (2002).
18. S. G. Nugent, D. Kumar, D. S. Rampton, D. F. Evans, Intestinal luminal pH in inflammatory bowel disease: Possible determinants and implications for therapy with aminosalicylates and other drugs. *Gut* **48**, 571–577 (2001).
19. F. E. Dewhirst, C. C. Chien, B. J. Paster, R. L. Ericson, R. P. Orcutt, D. B. Schauer, J. G. Fox, Phylogeny of the defined murine microbiota: Altered Schaedler flora. *Appl. Environ. Microbiol.* **65**, 3287–3292 (1999).
20. G. Dothel, M. R. Barbaro, H. Boudin, V. Vasina, C. Cremon, L. Gargano, L. Bellacosa, R. De Giorgio, C. Le Berre-Scoul, P. Aubert, M. Neunlist, F. De Ponti, V. Stanghellini, G. Barbara, Nerve fiber outgrowth is increased in the intestinal mucosa of patients with irritable bowel syndrome. *Gastroenterology* **148**, 1002–1011.e4 (2015).
21. G. Barbara, V. Stanghellini, R. De Giorgio, C. Cremon, G. S. Cottrell, D. Santini, G. Pasquinelli, A. M. Morselli-Labate, E. F. Grady, N. W. Bunnett, S. M. Collins, R. Corinaldesi, Activated mast cells in proximity to colonic nerves correlate with abdominal pain in irritable bowel syndrome. *Gastroenterology* **126**, 693–702 (2004).
22. G. Barbara, B. Wang, V. Stanghellini, R. de Giorgio, C. Cremon, G. Di Nardo, M. Trevisani, B. Campi, P. Geppetti, M. Tonini, N. W. Bunnett, D. Grundy, R. Corinaldesi, Mast cell-dependent excitation of visceral-nociceptive sensory neurons in irritable bowel syndrome. *Gastroenterology* **132**, 26–37 (2007).
23. V. Godot, M. Arock, G. Garcia, F. Capel, C. Flys, M. Dy, D. Emilie, M. Humbert, H4 histamine receptor mediates optimal migration of mast cell precursors to CXCL12. *J. Allergy Clin. Immunol.* **120**, 827–834 (2007).
24. O. Bednarska, S. A. Walter, M. Casado-Bedmar, M. Strom, E. Salvo-Romero, M. Vicario, E. A. Mayer, A. V. Keita, Vasoactive intestinal polypeptide and mast cells regulate increased passage of colonic bacteria in patients with irritable bowel syndrome. *Gastroenterology* **153**, 948–960.e3 (2017).
25. B. Schirmer, T. Rezniczek, R. Seifert, D. Neumann, Proinflammatory role of the histamine H4 receptor in dextrane sodium sulfate-induced acute colitis. *Biochem. Pharmacol.* **98**, 102–109 (2015).
26. J. B. Wechsler, A. Szabo, C. L. Hsu, R. A. Krier-Burris, H. A. Schroeder, M. Y. Wang, R. G. Carter, T. E. Velez, L. M. Aguiniga, J. B. Brown, M. L. Miller, B. K. Wershil, T. A. Barrett, P. J. Bryce, Histamine drives severity of innate inflammation via histamine 4 receptor in murine experimental colitis. *Mucosal Immunol.* **11**, 861–870 (2018).
27. A. Deiteren, J. G. De Man, N. E. Ruyssers, T. G. Moreels, P. A. Pelckmans, B. Y. De Winter, Histamine H4 and H1 receptors contribute to postinflammatory visceral hypersensitivity. *Gut* **63**, 1873–1882 (2014).
28. G. Major, S. Pritchard, K. Murray, J. P. Alappadan, C. L. Hoad, L. Marciani, P. Gowland, R. Spiller, Colon hypersensitivity to distension, rather than excessive gas production, produces carbohydrate-related symptoms in individuals with irritable bowel syndrome. *Gastroenterology* **152**, 124–133.e2 (2017).
29. S. D. Dorn, O. S. Palsson, S. I. Thiwan, M. Kanazawa, W. C. Clark, M. A. van Tilburg, D. A. Drossman, Y. Scarlett, R. L. Levy, Y. Ringel, M. D. Crowell, K. W. Olden, W. E. Whitehead, Increased colonic pain sensitivity in irritable bowel syndrome is the result of an increased tendency to report pain rather than increased neurosensory sensitivity. *Gut* **56**, 1202–1209 (2007).
30. R. Roka, J. Demaude, N. Cenac, L. Ferrier, C. Salvador-Cartier, R. Garcia-Villar, J. Fioramonti, L. Bueno, Colonic luminal proteases activate colonocyte proteinase-activated receptor-2 and regulate paracellular permeability in mice. *Neurogastroenterol. Motil.* **19**, 57–65 (2007).
31. A. Annahazi, L. Ferrier, V. Bezirard, M. Leveque, H. Eutamene, A. Ait-Belgnaoui, M. Coeffier, P. Ducrotte, R. Roka, O. Inczefi, K. Gecse, A. Rosztoczy, T. Molnar, T. Ringel-Kulka, Y. Ringel, T. Piche, V. Theodorou, T. Wittmann, L. Bueno, Luminal cysteine-proteases degrade colonic tight junction structure and are responsible for abdominal pain in constipation-predominant IBS. *Am. J. Gastroenterol.* **108**, 1322–1331 (2013).
32. J. Dionne, A. C. Ford, Y. Yuan, W. D. Chey, B. E. Lacy, Y. A. Saito, E. M. M. Quigley, P. Moayyedi, A systematic review and meta-analysis evaluating the efficacy of a gluten-free diet and a low FODMAPs diet in treating symptoms of irritable bowel syndrome. *Am. J. Gastroenterol.* **113**, 1290–1300 (2018).
33. J. L. Sonnenburg, F. Backhed, Diet-microbiota interactions as moderators of human metabolism. *Nature* **535**, 56–64 (2016).
34. S. M. Brierley, R. C. Jones III, G. F. Gebhart, L. A. Blackshaw, Splanchnic and pelvic mechanosensory afferents signal different qualities of colonic stimuli in mice. *Gastroenterology* **127**, 166–178 (2004).
35. C. Ibeakanma, F. Ochoa-Cortes, M. Miranda-Morales, T. McDonald, I. Spreadbury, N. Cenac, F. Cattaruzza, D. Hurlbut, S. Vanner, N. Bunnett, N. Vergnolle, S. Vanner, Brain-gut interactions increase peripheral nociceptive signaling in mice with postinfectious irritable bowel syndrome. *Gastroenterology* **141**, 2098–2108.e5 (2011).
36. I. Spreadbury, F. Ochoa-Cortes, C. Ibeakanma, N. Martin, D. Hurlbut, S. J. Vanner, Concurrent psychological stress and infectious colitis is key to sustaining enhanced peripheral sensory signaling. *Neurogastroenterol. Motil.* **27**, 347–355 (2015).
37. R. Thurmond, P. Dunford, W. Eckert, L. Karlsson, P. Ward, A. Greenspan. (2017).
38. R. L. Thurmond, J. Venable, B. Savall, D. La, S. Snook, P. J. Dunford, J. P. Edward, Clinical development of histamine H4 receptor antagonists. *Handb. Exp. Pharmacol.* **241**, 301–320 (2017).
39. R. L. Thurmond, J. Venable, B. Savall, D. La, S. Snook, P. J. Dunford, J. P. Edwards, Clinical development of histamine H4 receptor antagonists. *Handb. Exp. Pharmacol.* **241**, 301–320 (2017).
40. F. J. Whelan, M. G. Surette, A comprehensive evaluation of the sl1p pipeline for 16*S* rRNA gene sequencing analysis. *Microbiome* **5**, 100 (2017).
41. A. K. Bartram, M. D. Lynch, J. C. Stearns, G. Moreno-Hagelsieb, J. D. Neufeld, Generation of multimillion-sequence 16*S* rRNA gene libraries from complex microbial communities by assembling paired-end illumina reads. *Appl. Environ. Microbiol.* **77**, 3846–3852 (2011).
42. B. J. Callahan, P. J. McMurdie, M. J. Rosen, A. W. Han, A. J. A. Johnson, S. P. Holmes, DADA2: High-resolution sample inference from Illumina amplicon data. *Nat. Methods* **13**, 581–583 (2016).
43. E. Bolyen, J. R. Rideout, M. R. Dillon, N. Bokulich, C. C. Abnet, G. A. Al-Ghalith, H. Alexander, E. J. Alm, M. Arumugam, F. Asnicar, Y. Bai, J. E. Bisanz, K. Bittinger, A. Brejnrod, C. J. Brislawn, C. T. Brown, B. J. Callahan, A. M. Caraballo-Rodríguez, J. Chase, E. K. Cope, R. D. Silva, C. Diener, P. C. Dorrestein, G. M. Douglas, D. M. Durall, C. Duvallet, C. F. Edwardson, M. Ernst, M. Estaki, J. Fouquier, J. M. Gauglitz, S. M. Gibbons, D. L. Gibson, A. Gonzalez, K. Gorlick, J. Guo, B. Hillmann, S. Holmes, H. Holste, C. Huttenhower, G. A. Huttley, S. Janssen, A. K. Jarmusch, L. Jiang, B. D. Kaehler, K. B. Kang, C. R. Keefe,

P. Keim, S. T. Kelley, D. Knights, I. Koester, T. Kosciolek, J. Kreps, M. G. I. Langille, J. Lee, R. Ley, Y.-X. Liu, E. Loftfield, C. Lozupone, M. Maher, C. Marotz, B. D. Martin, D. M. Donald, L. J. McIver, A. V. Melnik, J. L. Metcalf, S. C. Morgan, J. T. Morton, A. T. Naimey, J. A. Navas-Molina, L. F. Nothias, S. B. Orchanian, T. Pearson, S. L. Peoples, D. Petras, M. L. Preuss, E. Pruesse, L. B. Rasmussen, A. Rivers, M. S. Robeson II, P. Rosenthal, N. Segata, M. Shaffer, A. Shiffer, R. Sinha, S. J. Song, J. R. Spear, A. D. Swafford, L. R. Thompson, P. J. Torres, P. Trinh, A. Tripathi, P. J. Turnbaugh, S. Ul-Hasan, J. J. J. van der Hooft, F. Vargas, Y. Vázquez-Baeza, E. Vogtmann, M. von Hippel, W. Walters, Y. Wan, M. Wang, J. Warren, K. C. Weber, C. H. D. Williamson, A. D. Willis, Z. Z. Xu, J. R. Zaneveld, Y. Zhang, Q. Zhu, R. Knight, J. G. Caporaso, Reproducible, interactive, scalable and extensible microbiome data science using QIIME 2. *Nat. Biotechnol.* **37**, 852–857 (2019).

44. Q. Wang, G. M. Garrity, J. M. Tiedje, J. R. Cole, Naive Bayesian classifier for rapid assignment of rRNA sequences into the new bacterial taxonomy. *Appl. Environ. Microbiol.* **73**, 5261–5267 (2007).
45. T. Z. DeSantis, P. Hugenholtz, N. Larsen, M. Rojas, E. L. Brodie, K. Keller, T. Huber, D. Dalevi, P. Hu, G. L. Andersen, Greengenes, a chimera-checked 16*S* rRNA gene database and workbench compatible with ARB. *Appl. Environ. Microbiol.* **72**, 5069–5072 (2006).
46. X. C. Morgan, B. Kabakchiev, L. Waldron, A. D. Tyler, T. L. Tickle, R. Milgrom, J. M. Stempak, D. Gevers, R. J. Xavier, M. S. Silverberg, C. Huttenhower, Associations between host gene expression, the mucosal microbiome, and clinical outcome in the pelvic pouch of patients with inflammatory bowel disease. *Genome Biol.* **16**, 67 (2015).
47. M. G. Langille, J. Zaneveld, J. G. Caporaso, D. McDonald, D. Knights, J. A. Reyes, J. C. Clemente, D. E. Burkepile, R. L. Vega Thurber, R. Knight, R. G. Beiko, C. Huttenhower, Predictive functional profiling of microbial communities using 16*S* rRNA marker gene sequences. *Nat. Biotechnol.* **31**, 814–821 (2013).
48. P. J. McMurdie, S. Holmes, phyloseq: An R package for reproducible interactive analysis and graphics of microbiome census data. *PLOS ONE* **8**, e61217 (2013).
49. P. Hemarajata, C. Gao, K. J. Pflughoeft, C. M. Thomas, D. M. Saulnier, J. K. Spinler, J. Versalovic, Lactobacillus reuteri-specific immunoregulatory gene rsiR modulates histamine production and immunomodulation by Lactobacillus reuteri. *J Bacteriol* **195**, 5567–5576 (2013).
50. P. Bercik, L. Wang, E. F. Verdu, Y. K. Mao, P. Blennerhassett, W. I. Khan, I. Kean, G. Tougas, S. M. Collins, Visceral hyperalgesia and intestinal dysmotility in a mouse model of postinfective gut dysfunction. *Gastroenterology* **127**, 179–187 (2004).
51. P. A. Lynn, L. A. Blackshaw, In vitro recordings of afferent fibres with receptive fields in the serosa, muscle and mucosa of rat colon. *J. Physiol.* **518**, 271–282 (1999).
52. S. J. Brookes, N. J. Spencer, M. Costa, V. P. Zagorodnyuk, Extrinsic primary afferent signalling in the gut. *Nat. Rev. Gastroenterol. Hepatol.* **10**, 286–296 (2013).
53. C. Ibeakanma, S. Vanner, TNFα is a key mediator of the pronociceptive effects of mucosal supernatant from human ulcerative colitis on colonic DRG neurons. *Gut* **59**, 612–621 (2010).
54. W. Stewart, D. J. Maxwell, Distribution of and organisation of dorsal horn neuronal cell bodies that possess the muscarinic m2 acetylcholine receptor. *Neuroscience* **119**, 121–135 (2003).
55. A. M. Bolger, M. Lohse, B. Usadel, Trimmomatic: A flexible trimmer for Illumina sequence data. *Bioinformatics* **30**, 2114–2120 (2014).
56. R. R. Wick, L. M. Judd, C. L. Gorrie, K. E. Holt, Unicycler: Resolving bacterial genome assemblies from short and long sequencing reads. *PLOS Comput. Biol.* **13**, e1005595 (2017).
57. A. Gurevich, V. Saveliev, N. Vyahhi, G. Tesler, QUAST: Quality assessment tool for genome assemblies. *Bioinformatics* **29**, 1072–1075 (2013).
58. R. R. Wick, M. B. Schultz, J. Zobel, K. E. Holt, Bandage: Interactive visualization of de novo genome assemblies. *Bioinformatics* **31**, 3350–3352 (2015).
59. T. Seemann, Prokka: Rapid prokaryotic genome annotation. *Bioinformatics* **30**, 2068–2069 (2014).
60. J. J. Davis, A. R. Wattam, R. K. Aziz, T. Brettin, R. Butler, R. M. Butler, P. Chlenski, N. Conrad, A. Dickerman, E. M. Dietrich, J. L. Gabbard, S. Gerdes, A. Guard, R. W. Kenyon, D. Machi, C. Mao, D. Murphy-Olson, M. Nguyen, E. K. Nordberg, G. J. Olsen, R. D. Olson, J. C. Overbeek, R. Overbeek, B. Parrello, G. D. Pusch, M. Shukla, C. Thomas, M. VanOeffelen, V. Vonstein, A. S. Warren, F. Xia, D. Xie, H. Yoo, R. Stevens, The PATRIC bioinformatics resource center: Expanding data and analysis capabilities. *Nucleic Acids Res.* **48**, D606–D612 (2020).
61. B. P. Alcock, A. R. Raphenya, T. T. Y. Lau, K. K. Tsang, M. Bouchard, A. Edalatmand, W. Huynh, A. V. Nguyen, A. A. Cheng, S. Liu, S. Y. Min, A. Miroshnichenko, H. K. Tran, R. E. Werfalli, J. A. Nasir, M. Oloni, D. J. Speicher, A. Florescu, B. Singh, M. Faltyn, A. Hernandez-Koutoucheva, A. N. Sharma, E. Bordeleau, A. C. Pawlowski, H. L. Zubyk, D. Dooley, E. Griffiths, F. Maguire, G. L. Winsor, R. G. Beiko, F. S. L. Brinkman, W. W. L. Hsiao, G. V. Domselaar, A. G. McArthur, CARD 2020: Antibiotic resistome surveillance with the comprehensive antibiotic resistance database. *Nucleic Acids Res.* **48**, D517–D525 (2020).
62. A. G. McArthur, N. Waglechner, F. Nizam, A. Yan, M. A. Azad, A. J. Baylay, K. Bhullar, M. J. Canova, G. De Pascale, L. Ejim, L. Kalan, A. M. King, K. Koteva, M. Morar, M. R. Mulvey, J. S. O'Brien, A. C. Pawlowski, L. J. Piddock, P. Spanogiannopoulos, A. D. Sutherland, I. Tang, P. L. Taylor, M. Thaker, W. Wang, M. Yan, T. Yu, G. D. Wright, The comprehensive antibiotic resistance database. *Antimicrob. Agents Chemother.* **57**, 3348–3357 (2013).
63. S. C. Bayliss, H. A. Thorpe, N. M. Coyle, S. K. Sheppard, E. J. Feil, PIRATE: A fast and scalable pangenomics toolbox for clustering diverged orthologues in bacteria. *Gigascience* **8**, (2019).
64. A. J. Page, C. A. Cummins, M. Hunt, V. K. Wong, S. Reuter, M. T. Holden, M. Fookes, D. Falush, J. A. Keane, J. Parkhill, Roary: Rapid large-scale prokaryote pan genome analysis. *Bioinformatics* **31**, 3691–3693 (2015).
65. M. J. Hossain, C. M. Thurlow, D. Sun, S. Nasrin, M. R. Liles, Genome modifications and cloning using a conjugally transferable recombineering system. *Biotechnol. Rep. (Amst.)* **8**, 24–35 (2015).
66. K. A. Datsenko, B. L. Wanner, One-step inactivation of chromosomal genes in *Escherichia coli* K-12 using PCR products. *Proc. Natl. Acad. Sci. U.S.A.* **97**, 6640–6645 (2000).
67. J. Um, D. G. Kim, M. Y. Jung, G. D. Saratale, M. K. Oh, Metabolic engineering of *Enterobacter aerogenes* for 2,3-butanediol production from sugarcane bagasse hydrolysate. *Bioresour. Technol.* **245**, 1567–1574 (2017).
68. P. J. Turnbaugh, R. E. Ley, M. A. Mahowald, V. Magrini, E. R. Mardis, J. I. Gordon, An obesity-associated gut microbiome with increased capacity for energy harvest. *Nature* **444**, 1027–1031 (2006).
69. N. M. Moreau, S. M. Goupry, J. P. Antignac, F. J. Monteau, B. J. Le Bizec, M. M. Champ, L. J. Martin, H. J. Dumon, Simultaneous measurement of plasma concentrations and 13C-enrichment of short-chain fatty acids, lactic acid and ketone bodies by gas chromatography coupled to mass spectrometry. *J. Chromatogr. B Analyt. Technol. Biomed. Life Sci.* **784**, 395–403 (2003).
70. T. H. Farncombe, Software-based respiratory gating for small animal conebeam CT. *Med. Phys.* **35**, 1785–1792 (2008).
71. R. Guerrero-Alba, E. E. Valdez-Morales, N. N. Jimenez-Vargas, C. Lopez-Lopez, J. Jaramillo-Polanco, T. Okamoto, Y. Nasser, N. W. Bunnett, A. E. Lomax, S. J. Vanner, Stress activates pronociceptive endogenous opioid signalling in DRG neurons during chronic colitis. *Gut* **66**, 2121–2131 (2017).
72. E. Valdez-Morales, R. Guerrero-Alba, F. Ochoa-Cortes, J. Benson, I. Spreadbury, D. Hurlbut, M. Miranda-Morales, A. E. Lomax, S. Vanner, Release of endogenous opioids during a chronic IBD model suppresses the excitability of colonic DRG neurons. *Neurogastroenterol. Motil.* **25**, 39–46.e4 (2013).
73. B. A. Moore, T. M. Stewart, C. Hill, S. J. Vanner, TNBS ileitis evokes hyperexcitability and changes in ionic membrane properties of nociceptive DRG neurons. *Am. J. Physiol. Gastrointest. Liver Physiol.* **282**, G1045–G1051 (2002).
74. C. Shimbori, C. Upagupta, P. S. Bellaye, E. A. Ayaub, S. Sato, T. Yanagihara, Q. Zhou, A. Ognjanovic, K. Ask, J. Gauldie, P. Forsythe, M. R. J. Kolb, Mechanical stress-induced mast cell degranulation activates TGF-β1 signalling pathway in pulmonary fibrosis. *Thorax* **74**, 455–465 (2019).
75. I. Khambati, S. Han, D. Pijnenburg, H. Jang, P. Forsythe, The bacterial quorum-sensing molecule, *N*-3-oxo-dodecanoyl-L-homoserine lactone, inhibits mediator release and chemotaxis of murine mast cells. *Inflamm. Res.* **66**, 259–268 (2017).

Funding: This study was funded by the Canadian Institutes of Health Research (CIHR) Foundation grant no. 143253 (to P.B. and S.M.C.), CIHR Operating grant no. 153231 (to S.V. and D.R.), and Canadian Association of Gastroenterology–CIHR Postdoctoral Fellowship #2014-2016 (to G.D.P.). **Author contributions:** G.D.P., P.B., S.J.V., D.E.R., and S.M.C. conceived and designed the study. G.D.P. performed mouse experiments (all colonizations and CT scans), bacterial culture experiments and isolations, RNA extractions, and data analysis, including 16*S* rRNA and Nanostring sequencing data. G.D.P. engineered *E. coli* to express the *hdc* gene. J.L., M.P., and C.S. contributed to mouse experiments. C.S., L.B., and A.M. performed immunohistochemistry and quantitative polymerase chain reaction (qPCR) of colon tissues, and C.S. analyzed the data. C.S. and L.B. performed and analyzed experiments with bone marrow–derived mast cells. V.R. performed and analyzed *hdc* gene experiments and created the MQ^{-hdc} mutant. P.B., G.D.P., X.B., and J.P performed in vivo visceromotor response experiments. Y.Z., Y.Y., N.J.-V., J.S., C.L.-L., and J.J.-P. performed and analyzed electrophysiology experiments. D.E.R., S.J.V., A.E.L., and M.B. analyzed and interpreted electrophysiology data. M.I.P.-S. conducted the longitudinal clinical study. E.F.V. provided germ-free mice and support for gnotobiotic experiments. G.D.P., P.B., C.S., S.J.V., S.M.C., and D.E.R. wrote and reviewed the manuscript. E.F.V., K.M., AE.L., and M.B. critically reviewed the manuscript. **Competing interests:** S.C. is a paid member of the Microbiome Advisory board for Norgine. The other authors declare that they have no competing interests. **Data and materials availability:** All data associated with this study are present in the paper or the Supplementary Materials. The 16*S* rRNA sequencing data have been deposited at National Center for Biotechnology Information BioProject no. PRJNA542489.

Submitted 26 April 2021
Resubmitted 24 November 2021
Accepted 24 March 2022
Published 27 July 2022
10.1126/scitranslmed.abj1895

Abstract

One-sentence summary: Bacterial histamine induces visceral hyperalgesia through H4 receptor–dependent pathways in a subset of patients with chronic abdominal pain.

Editor's Summary:
A role for bacterial histamine in abdominal pain

Gut bacteria have been implicated in the genesis of chronic pain disorders; however, the underlying mechanisms remain unclear. In new work, De Palma and colleagues show that histamine, a known neuroimmune modulator, is produced by gut bacteria and that it induces abdominal pain in a mouse model of irritable bowel syndrome (IBS). Bacterial histamine acts by attracting mast cells to the colon through activation of the histamine 4 receptor. The authors identified *Klebsiella aerogenes*, present in the gut microbiota of many patients with IBS, as the main bacterial producer of histamine. These results suggest that bacterial histamine may be a therapeutic target for treating chronic abdominal pain.